Journal of proteome research

pubs.acs.org/jpr Article

# Carbon Metabolism and the ROS Scavenging System Participate in *Nostoc flagelliforme*'s Adaptive Response to Dehydration Conditions through Protein Acetylation

Lingxia Wang,[§] Xiaoxu Li,[§] Meng Wang, Xiaorong Ma, Fan Song, Jinhong Hu, Wangli Liang, and Wenyu Liang*

Cite This: *J. Proteome Res.* 2022, 21, 482−493 Read Online

ACCESS | Metrics & More | Article Recommendations | Supporting Information

**ABSTRACT:** Acetylation represents an extensively occurring protein post-translational modification (PTM) that plays a key role in many cellular physiological and biochemical processes. However, studies on PTMs such as acetylation of lysine (LysAc) in cyanobacteria are still rare. In this study, a quantitative LysAc approach (acetylome) on the strains of *Nostoc flagelliforme* subjected to different dehydration treatments was conducted. We observed that starch contents were significantly accumulated due to dehydration treatments, and we identified 2474 acetylpeptides and 1060 acetylproteins based on acetylome analysis. Furthermore, an integrative analysis was performed on acetylome and nontargeted metabolism, and the results showed that many KEGG terms were overlapped for both omics analyses, including starch and sucrose metabolism, transporter activity, and carbon metabolism. In addition, time series clustering was analyzed, and some proteins related to carbon metabolism and the ROS scavenging system were significantly enriched in the list of differentially abundant acetylproteins (DAAPs). These protein expression levels were further tested by qPCR. A working model was finally proposed to show the biological roles of protein acetylation from carbon metabolism and the ROS scavenging system in response to dehydration in *N. flagelliforme*. We highlighted that LysAc was essential for the regulation of key metabolic enzymes in the dehydration stress response.

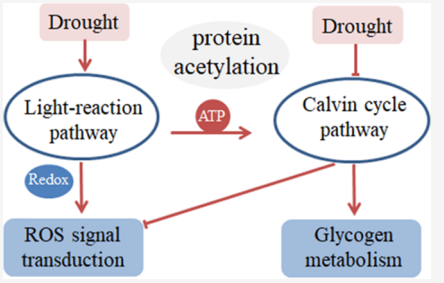


**KEYWORDS:** *Nostoc flagelliforme, protein acetylation, dehydration treatments, carbon metabolism, ROS scavenge*

## INTRODUCTION

Lysine acetylation (LysAc), as one of the major post-translational modifications (PTMs) of proteins, participates in many different biological processes and alters the protein function by changing the stability, cellular localization, and enzymatic activity of proteins. LysAc including histone and non-histone acetylation modification, a particularly dynamic and reversible type of PTM, is critical to uncover regulatory mechanisms of biological processes induced by various abiotic stresses in plants.[1,2] It is well known that LysAc was first discovered as a PTM type of histone; therefore, histone LysAc plays a crucial role in chromatin remodeling and transcription activation in the nucleus.[3−6] The studies of LysAc have broadened to an increasing number of proteins and reported that acetylation modifying enzymes were involved in almost all biological processes and biochemical reactions.[7,8]

The recent results have shown that LysAc is a widespread and conserved PTM from prokaryotes to eukaryotes.[8] The modification type exists in a large number of proteins biological function in diverse species, such as eubacteria, fungi, plants, and mammals.[9−12] It was reported that there are 776 acetylated sites in 513 identified proteins in the cyanobacterium *Synechocystis* sp. PCC 6803[13] and 1653 acetylated sites in 802 proteins in *Synechococcus* sp. PCC 7002.[9,13] In *Salmonella*, LysAc is widespread in the central metabolic enzymes and the occurrence of LysAc relates with the changes of carbon fluxes.[14] In mammalian, LysAc is especially enriched in protein complexes where it controls protein−protein interactions and enzymatic activities.[15]

In higher plants, LysAc is an important PTM in different photosynthesis-related proteins, such as the catalytic function of photosystem II (PSII) subunits, photosystem II (PSII) manganese-stabilizing protein (PsbO), light-harvesting chlorophyll a/b-binding proteins, ribulose-1,5-bisphosphate carboxylase/oxygenase (Rubisco), GAPDH, and other Calvin cycle enzymes.[9,16,17] Especially, LysAc denotes an important mechanism in the regulation of the Rubisco large subunit, in terms of its tertiary structure formation and catalytic function in photosynthesis.[16] In addition, the tricarboxylic acid (TCA)

**Received:** October 15, 2021
**Published:** January 12, 2022

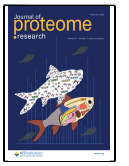







https://doi.org/10.1021/acs.jproteome.1c00823
*J. Proteome Res.* 2022, 21, 482−493

cycle, glycolysis, and pentose phosphate pathway were all regulated through LysAc for desirable energy supply to cells in plants.[11] Therefore, protein LysAc plays many crucial roles not only in epigenetic regulation of gene expression but also in the control of metabolic enzyme activity. Acetylation modification affects enzyme function probably by altering protein folding conformation.[18] These findings suggest that LysAc might have an extensive regulatory role for central metabolic levels.

*N. flagelliforme*, an extremophile belonging to the cyanobacterium, represents well thrives in extraordinary desiccation conditions. To date, proteome and transcriptome analyses have revealed the dynamic changes in the intermediate metabolism responses of *N. flagelliforme* in response to desiccation conditions, especially photosynthetic and carbohydrate metabolisms,[19−21] but how PTMs participate in the regulatory response of *N. flagelliforme* for adaption to dehydration stress conditions and what are their roles in the regulation of proteins remain unknown. Some metabolic pathways such as the photoreaction process and carbon assimilation metabolism were significantly enriched in the list of LysAc proteins, and these metabolic pathways could play key regulatory roles in central metabolic processes in cyanobacteria.[9,13] Because LysAc targets almost all cellular processes, maybe this modification has been related to *N. flagelliforme* desiccation-tolerant. Almost nothing is known about this modification in *N. flagelliforme*; thus, how LysAc regulates metabolic enzymes in *N. flagelliforme* in response to desiccation conditions needs to be studied further.

In this study, we focus on the acetylation regulatory mechanism of a specific cellular process including the carbon metabolic pathway and ROS signal transduction and intermediary metabolism caused by dehydration treatment in *N. flagelliforme*. We observed that this stress condition stimulates some post-translational modifications such as acetylation; therefore, we performed a combined analysis on acetylome and nontargeted metabolism. An extensive informatics analysis on differentially abundant acetylproteins (DAAPs) and differentially abundant metabolites (DAMs) was provided induced by dehydration treatments. Finally, we proposed a working model to illustrate the biological roles of acetylation regulation of carbon metabolism-related proteins in response to dehydration treatments in *N. flagelliforme*. This study paves the path for the molecular mechanism of rapid recovery from dehydration treatments in *N. flagelliforme*.

## MATERIALS AND METHODS

### Plant Materials

The *N. flagelliforme* strain, used in this study was collected from the Helan mountain east region (38.41′N, 105.95′E) of Ningxia in China. The sample cultivation was carried as described earlier.[21] Briefly, ∼0.5 g of dry weight samples were distributed equably and cultured in a greenhouse at 25 ± 2 °C with 400 $\mu$mol $m^{-2}$ $s^{-1}$ light intensity. To obtain a desiccated sample, colonies determined its weight at intervals of 10 min to evaluate water loss, defined as 0, 30, 75, and 100%. The parameter of water loss was determined as reported previously.[22]

### Enzyme Activities and Starch Determination

To uncover the effects of dehydration treatments on sucrose metabolism, we determined the activities of enzymes related to the sucrose biosynthesis pathway, including glycogen phosphorylase (GPa), glycogen synthetase (GCS), triose-phosphate isomerase (TPI), Rubisco, and fructose-1,6-bisphosphate aldolase (FBA). The activities of these enzymes were determined via an ELISA-based measurement kit produced by Suzhou Comin Biotech Co., Ltd. The product IDs for GPa, GCS, TPI, Rubisco, and FBA were GPA-1-Y, GCS-1-Y, TPI-1-G, RUBPS-1-Y, and FBA-1-G, respectively. The procedure of each enzyme activity measurement was conducted following the standard protocol. The samples were extracted with a pre-cold ball mill at 30 Hz for 5 min and were centrifuged at 12 000 rpm at 4 °C for 10 min; the supernatant was used to detect the enzyme activity at a wavelength of 340 nm. Starch contents were determined based on anthracenone colorimetry as documented previously.[23] The protein concentration was determined by the Bradford method.[24]

### Protein Extraction

The procedure of *N. flagelliforme* protein extraction was used based on the improved TCA method as our previous study reported.[20] The protein concentration was determined by the Bradford method.[24] The protein solution was used immediately for further experiments or protein pellets stored in −80 °C until use.

### Protein Trypsin Digestion and Lys-Acetylated Peptide Enrichment

The proteins were first treated with 10 mM DTT at 37 °C for 2.5 h and were then alkylated with 50 mM iodoacetamide (IAA) for 30 min at 37 °C in darkness. For trypsin digestion, the samples were incubated with a 1.5 M urea concentration. Then, the proteins were digested via trypsin for 18 h. After that, peptides were desalted by an SPE C18 column (Waters WAT051910) and vacuum-dried. To enrich LysAc peptides, tryptic peptide fractions were dissolved in buffer (50 mM MOPS/NaOH pH 7.2, 10 mM $Na_2HPO_4$, 50 mM NaCl). Then, the dissolved peptides were incubated with anti-LysAc antibody beads (PTMScan Acetyl-Lysine Motif Kit, Cell Signal Technology) to enrich the acetylated peptides.

### Proteomics Determination

The enriched peptides as described above were identified via a Q Exactive mass spectrometer (Thermo Fisher Scientific) with an easy nLC-1000 system (Thermo Fisher Scientific). In brief, the peptides were first loaded onto an RP-C18 column (Thermo EASY column SC001 traps) and separated using an analytical column (EASY column SC200 150 $\mu$m × 100 mm (RP-C18)) at a flow rate of 0.3 $\mu$L/min at a linear gradient ranging from 0 to 55% solvent B (0.1% FA in 84% ACN) over 110 min, then 55−100% over 8 min, and lastly remained at 100% for 2 min. The resulting peptides were analyzed with the Q Exactive mass spectrometer (Thermo Scientific). For MS scans, the $m/z$ scan ranges from 350 to 1800. Survey scans were acquired at a resolution of 60 000 at 210 $m/z$, and resolution for HCD spectra was set to 12 000 at 200 $m/z$.

### Bioinformatics Annotation Analysis

The mass spectrometry data were recorded via MaxQuant software equipped with the integrated Andromeda search engine (v. 1.3.0.5) against P17036_NCBI_Nostoc_ flagelliforme_18909_20171228.fasta. The thresholds of the false rate of acetylation modification sites were maintained at 0.02. To obtain high-confidence results, the baseline of the peptide length was set at 7 amino acids with LysAc site localization probability greater than 0.75. Motif-x software was used for model sequence analysis constituted with amino acids in particular positions of modifier-13-mers in all protein


https://doi.org/10.1021/acs.jproteome.1c00823
J. Proteome Res. 2022, 21, 482−493

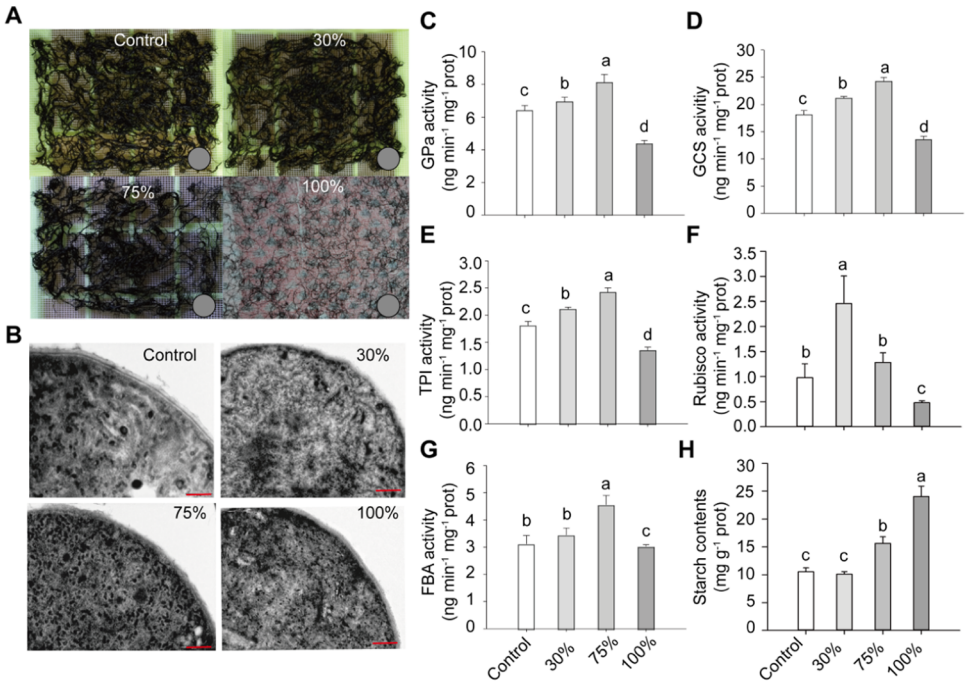


**Figure 1.** Changes in the morphology and activities of sucrose metabolic pathways of *N. flagelliforme* exposed to different dehydration treatments. (A) Images of dehydration treatments in *N. flagelliforme* (0, 30, 75, and 100%). (B) Images of transmission electron microscopy of *N. flagelliforme* exposed to different dehydration treatments. (C−H) Activities of enzymes related to the sucrose biosynthesis pathway, including glycogen phosphorylase (GPa) (C), glycogen synthetase (GCS) (D), triose-phosphate isomerase (TPI) (E), ribulose-1,5-bisphosphate carboxylase/oxygenase (Rubisco) (F), fructose-1,6-bisphosphate aldolase (FBA) (G), and starch content (H). Different alphabetic letters represent significant levels at $P < 0.05$ based on one-way ANVOA. Values are mean± standard deviation. $n = 3$.

sequences. The minimum occurrence was 50; the significance threshold was set at 0.00018.

We performed gene ontology (GO) annotation of all acetylproteins using Blast2GO software.[25] To identify the enriched metabolic pathways of the differentially expressed protein (DEP) against all identified proteins, we performed Kyoto Encyclopaedia of Genes and Genomes (KEGG) analysis by Fisher's Exact Test ($P$-value <0.05). The mass spectrometry proteomics data were deposited to the ProteomeXchange Consortium via the PRIDE[26] partner repository with the data set identifier PXD029765.

## LC-MS/MS-Based Metabolism Determination

Nontargeted metabolic profiling in the *N. flagelliforme* strain was performed based on Q Exactive, LC-MS/MS (Thermo Scientific). We first extracted the *N. flagelliforme* samples with a metal ball mill at 35 Hz for at least 5 min, and then dissolved these samples with 1.6 mL of methanol/chloroform and kept them at −20 °C for 6 h. The mixture was centrifuged at 2000*g* at 4 °C for at least 10 min and then was filtered with 0.43 μm of organic-phase medium (GE Healthcare, 6789-0404). Metabolomics analysis was performed by Metabolon (Durham, NC). We identified these metabolites by detecting their retention times and mass spectra with reference compounds according to the mass spectra libraries NIST02 and Golm metabolome database (http://csbdb.mpimp-golm.mpg.de/csbdb/gmd/gmd.html).

## qRT-PCR Analysis

The total RNA was extracted through an RNAprep Pure Kit (TIANGEN) following the standard instruction;[5] ∼1 μg of the total RNA was reverse-transcribed with the PrimeScript RT reagent Kit (TakaRa) following the manufacturer's instructions. We performed qRT-PCR using 16s rRNA as a housekeeping gene. The genes were detected including malate dehydrogenase (*MDH*), class II fructose-bisphosphatase (*GLPX*), Rubisco small subunit 3 (*RbcS3*), F0F1 ATP synthase subunit B′ (*ATPG*), pyruvate dehydrogenase (acetyl-transferring) E1 component subunit (*PDHA*), class 1 fructose-bisphosphatase (*FBP1*), glycogen debranching enzyme (*GLGX*), photosystem I reaction center subunit X (*PsaK*), glucose-1-phosphate adenylyl transferase (*GlgC*), isocitrate dehydrogenase 1 (*IDH*), phosphoglycerate kinase (*PGK*), superoxide dismutase (*SOD*), glutathione S-transferase (*GST*), and glutathione synthase 1 (*GS1*). The primers for each gene are listed in Table S1. In addition, the expression levels of genes were quantified with the CFX96 real-time quantitative PCR system. The relative mRNA level was calculated using the $2^{-\Delta\Delta Ct}$ method.[27] All assays used for qRT-PCR were performed at least three biological replicates and three technical replicates for each biological sample.

## Transmission Electron Microscopy

The samples of the *N. flagelliforme* strain for transmission electron microscopy (TEM) were first fixed in a mixture of 2.5% v/v glutaraldehyde in 0.05 M sodium cacodylate trihydrate buffer (pH 7.0) for 3 h and then fixed in 1% w/v $OsO_4$ for 12 h at 4 °C, dehydrated in a graded acetone series, and embedded in epoxy resin Epon812. Ultrathin sections (70-80 nm) on grids were stained with both lead citrate and uranyl acetate and viewed with an electron microscope (JEM-1200HC) as documented previously.[20]

## Statistical Analysis

The experiments conducted in the current study were carried out with at least three biological replications. The data from


https://doi.org/10.1021/acs.jproteome.1c00823
J. Proteome Res. 2022, 21, 482−493

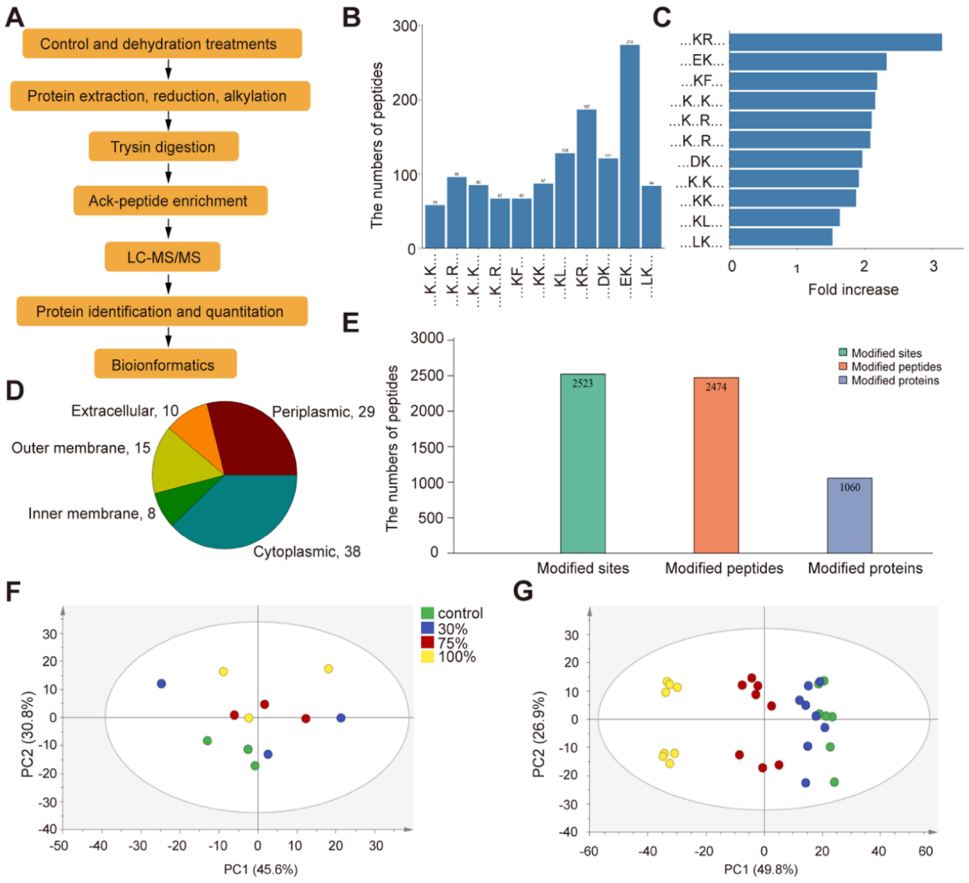


**Figure 2.** Pipeline of proteomic-based acetylation for proteins in *N. flagelliforme* exposed to different dehydration treatments. (A) Pipeline of acetylome analysis performed in this study. (B, C) Numbers and fold increase of major types of enriched motifs obtained from acetylpeptides. (D) Cellular distribution of aetylpeptides. (E) Numbers of modified (acetylated) sites, peptides, and annotated proteins. (F, G) Principal component analysis on proteomics and nontargeted metabolism, respectively. Letters in the legend for panels (F) and (G) represent different dehydration treatments from 0 to 100%.

metabolic, enzyme activities, and gene expression experiments were shown as mean ± standard deviation (SD). The differential comparison among different dehydration-treated groups was performed by one-way ANOVA analysis.

## RESULTS

### Performance of *N. flagelliforme* Subjected to Different Dehydration Treatments

In this study, a dehydration treatment was applied to *N. flagelliforme* samples (Figure 1A). The result shows that no obvious changes in the cell structure and the thylakoid membrane structure of *N. flagelliforme* samples occurred due to dehydration treatments as shown by transmission electron microscopy (TEM) imaging (Figure 1B). We also observed that the activities of some enzymes related to the sucrose biosynthetic pathway were upregulated under moderate dehydration treatments (30 and 75%), such as GPa, GCS, TPI, Rubisco, and FBA (Figure 1C−G). In addition, we observed that starch contents were significantly accumulated induced by dehydration treatments (Figure 1H).

### Detection of Lysine Acetylation and Metabolites in *N. flagelliforme*

We then identified acetylome in *N. flagelliforme* subjected to different dehydration treatments to uncover the effects of PTMs on responsive regulation in *N. flagelliforme*. To obtain sufficient numbers of acetylated peptides (acetylpeptides) identified, a modified protocol was performed for acetylpeptides antibody enrichment as well as high pH reversed-phase peptide fractionation after trypsin digestion (Figure 2A). As a result, most of the acetylpeptides containing EK and KR motifs were enriched (Figure 2B). The fold increase of acetylated proteins (acetylproteins) containing KR motifs was greater than that containing LK motifs due to dehydration stress treatments in *N. flagelliforme* (Figure 2C). Large proportions (38%) of acetylproteins are located in the cytoplasm and 23% of acetylproteins exist in the membrane, while 29 and 10% of acetylproteins are located in the periplasmic and extracellular regions, respectively (Figure 2D). Furthermore, we found that 43% of the modified proteins that accounted for 2474 identified acetylpeptides were annotated (Figure 2E). Principal component analysis (PCA) on the relative abundance of each metabolite and acetylprotein across all *N. flagelliforme* samples reveals that the samples within each treatment from different dehydration treatments were clearly clustered for metabolism analysis, but not for acetylome analysis (Figure 2F−G).

### Identification of Aacetylpeptides via LC-MS/MS

As mentioned above, we successfully identified 2474 acetylpeptides, and these peptides were corresponded to 1060 acetylproteins in *N. flagelliforme* (Figure 2E). The mass error represents the differences between predicted *m*/*z* scores and observed *m*/*z* scores for acetylpeptides identified, the major proportion of which ranges from −2 to 2 (Figure S1A),


https://doi.org/10.1021/acs.jproteome.1c00823
J. Proteome Res. 2022, 21, 482−493

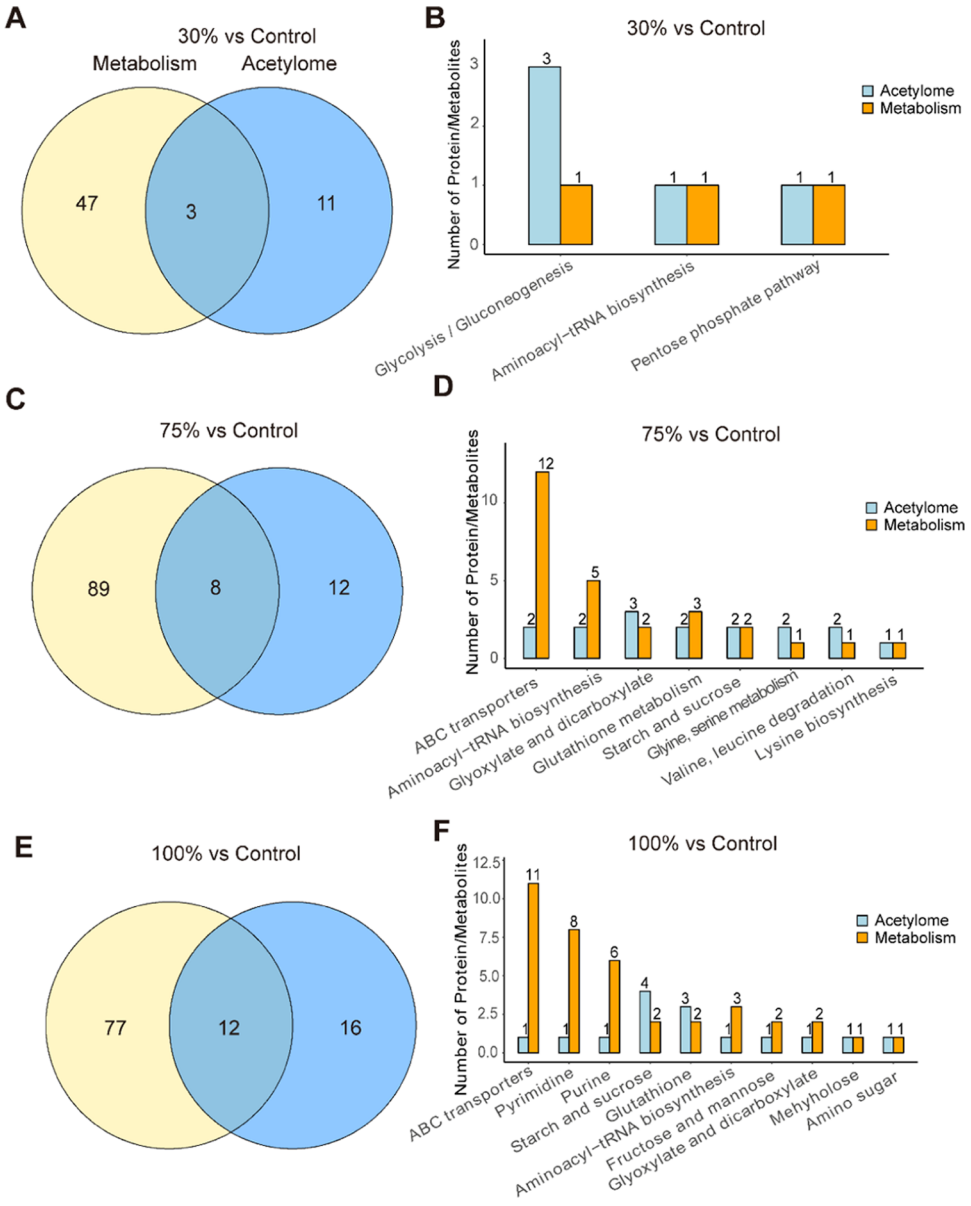


**Figure 3.** Integrative analysis on metabolism and acetylated modified proteomics in *N. flagelliforme* exposed to different dehydration treatments. The Venn diagram represents the overlapped KEGG pathways for differentially abundant lys-acetylated proteins (DAAPs) and differentially abundant metabolites (DAMs) for comparison of 30% and control (A), 75% and control (C), and 100% and control (E). The detailed numbers of overlapped KEGG pathways for both DAAPs and DAMs for comparison of 30% and control (B), 75% and control (D), and 100% and control (F).

and the median score for acetylpeptides is 102.52, and the percentage of acetylpeptides with more than 60 ion score is 88.31% (Figure S1B). The acetylpeptide ratio yields normal distribution (Figure S2A), and in addition, the molecular weight of most acetylproteins identified ranges from 30 to 40 kDa (Figure S2B), suggesting that lysine acetylation is an important type of PTM that occurs in non-histone proteins of *N. flagelliforme* proteins except for histones. Most of the peptides identified ranged from 7 to 17 amino acids in length, and the remaining peptides (more than 11%) were longer than 17 amino acids (Figure S3A). Regarding the acetylproteins identified, arginine (R) was highly enriched at the +1 (log 2) position in *N. flagelliform*, while leucine (L) was most commonly found at the +1(log 2) and +2 (log 2) positions. Glutamate (E) appears more frequently at the −1(log2) position, with a 2.93% average frequency (Figure S3B). The coverage of acetylpeptides mapped to the acetylproteins is high for some proteins related to the photosynthetic process. For example, the Ribulose bisphosphate carboxylase large subunit (RbcL, WP_100900845.1) involved in carbon fixation was observed with 13 LysAc sites. We identified 1515 overlapped acetylpeptides and 733 overlapped acetylproteins for *N. flagelliforme* across different dehydration treatments (Figure S4A−B).

## Integrative Analysis between Acetylproteomic and Metabolites

To learn the molecular profilings in *N. flagelliforme* subjected to different dehydration treatments, we performed an integrative analysis between proteome and metabolism. KEGG pathway enrichment analyses suggest that there are 3, 8, and 12 overlapped KEGG pathways for 30% dehydration versus control, 75% dehydration versus control, and 100% dehydration versus control, respectively (Figure 3A,C,E). The


https://doi.org/10.1021/acs.jproteome.1c00823
J. Proteome Res. 2022, 21, 482−493

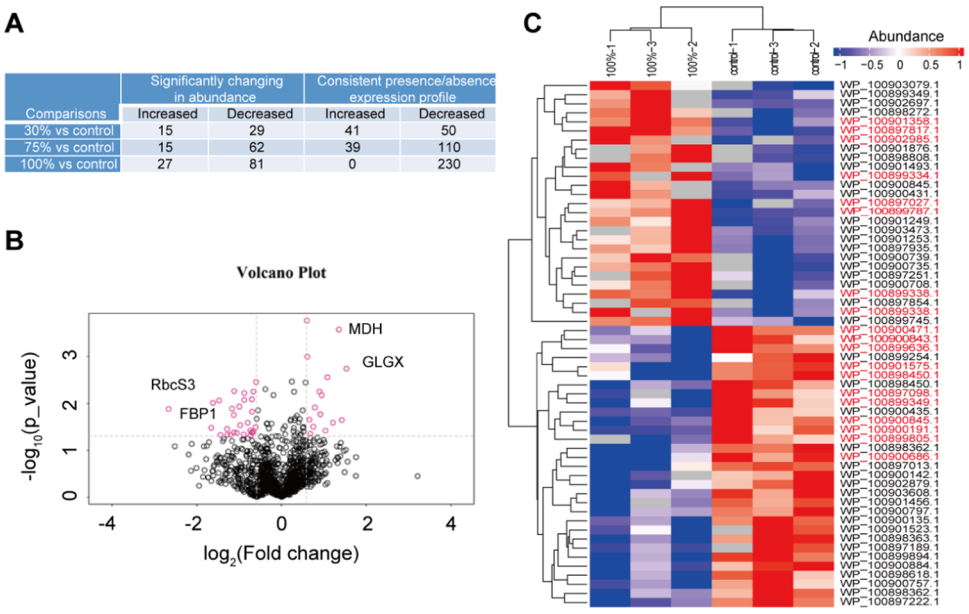


**Figure 4.** Differentially abundant proteins for different comparisons of dehydration treatments and control. (A) Differentially abundant acetylproteins (DAAPs) caused by dehydration treatments in *N. flagelliforme*. (B) Volcano plot represents significant DAAPs. (C) Heatmap representing the top 50% significant DAAPs. Significant LysAc levels across three dehydration treatments relative to control based on one-way ANOVA are highlighted in red. The list of these DAAPs is shown in Table S3.

corresponding overlapped KEGG pathways are related to carbon metabolism (including glycolysis/gluconeogenesis, anlnoacyl-tRNA biosynthesis, and pentose phosphate pathway) for 30% dehydration treatments compared to control, and carbon metabolism pathways (including glyxyolate and dicarboxylate metabolism, glutathione metabolism, starch and sucrose metabolism, valine, leucine, and isoleucine degradation, and glycine, serine, and threonine metabolism) for 75% dehydration compared to control (Figure 3B,D). In addition, for 100% dehydration compared to control, we found that most overlapped KEGG pathways are involved in sucrose-related metabolism pathways, such as starch and sucrose metabolism, glutathione metabolism, fructose and mannose metabolism, and glyoxylate and dicarboxylate metabolism (Figure 3F).

## Dehydration-Induced DAAPs and DAMs in *N. flagelliforme*

Furthermore, we analyzed the up-/downregulated DAAPs and DAMs for different comparisons of dehydration and control. Two to four times more downregulated DAAPs were observed than upregulated DAAPs across different comparisons of dehydration and control (Figures 4A and S5−S7). In particular, for extreme dehydration treatments (100% vs control), we found three times more downregulated DAAPs as well as DAMs, indicating the stressful conditions for *N. flagelliforme* in this case (Figures 4B and S7). The top 50% downregulated DAAPs followed by prolonged dehydration treatments from 30 to 100% were presented, including RbcS3 and FBP1, and some upregulated DAAPs were presented such as MDH and GLGX (Figure 4B,C and Table S3).

## Time Series Clustering Analysis on DAAPs and DAMs

The results of time series clustering analysis show that the abundance of most acetylproteins gradually decreased following prolonged dehydration treatments (Figure S8). Based on one-way ANOVA, we determined DAAPs across different dehydration treatments. In this manner, we performed GO and KEGG analysis on the list of DAAPs among different dehydration treatments (Figure 5). The results show that biological pathways related to photosynthesis, pyridine nucleotide metabolism, magnesium ion binding, oxidoreduction coenzyme metabolism, and oxidoreductase activity were significantly enriched in the list of DAAPs in response to dehydration treatments in *N. flagelliforme* (Figure 5A).

For KEGG analysis, we found that the pathways of primary metabolism, photorespiration, and amino sugar metabolism were significantly enriched in the list of DAMs. These detailed KEGG terms include photosynthesis, oxidative phosphorylation, glutathione metabolism, glycolysis/gluconeogenesis, citrate cycle, pentose phosphate pathway, starch and sucrose metabolism, fructose and mannose metabolism, glyoxylate and dicarboxylate metabolism, and photosynthesis-antenna proteins (Figure 5B). Most metabolites related to amino acid and sucrose metabolism show a gradual increase following prolonged dehydration treatments, such as glutamate, trehalose, glutamine, proline, and sucrose (Figure 6).

## Predicted Protein−Protein Interaction Analysis

Furthermore, we tested the relative expression levels of the genes related to carbon metabolism and glutathione metabolism and found that the expression levels for only a few genes exhibit a gradual increase following different dehydration treatments, such as *MDH* and *GLGX* (Figures 7A andS9A). In contrast, most genes are downregulated followed by dehydration effects, such as *RbcS3*, *ATPB*, *PDHA*, *FBP1*, *PsaK*, *GlgC*, *IDH*, and *PGK* (Figures 7B−F and S9B−E). Importantly, some genes related to antioxidant systems are slightly or dramatically downregulated followed by dehydration effects (Figure S9F−H), such as *SOD*, *GST*, and *GS1*. The close correlations among these genes were supported by a reconstructive gene regulation network (Figure S10).

Finally, we proposed the working model representing the biological roles of LysAc levels of DAAPs in *N. flagelliforme* subjected to different dehydration treatments. First, LysAc


https://doi.org/10.1021/acs.jproteome.1c00823
J. Proteome Res. 2022, 21, 482−493

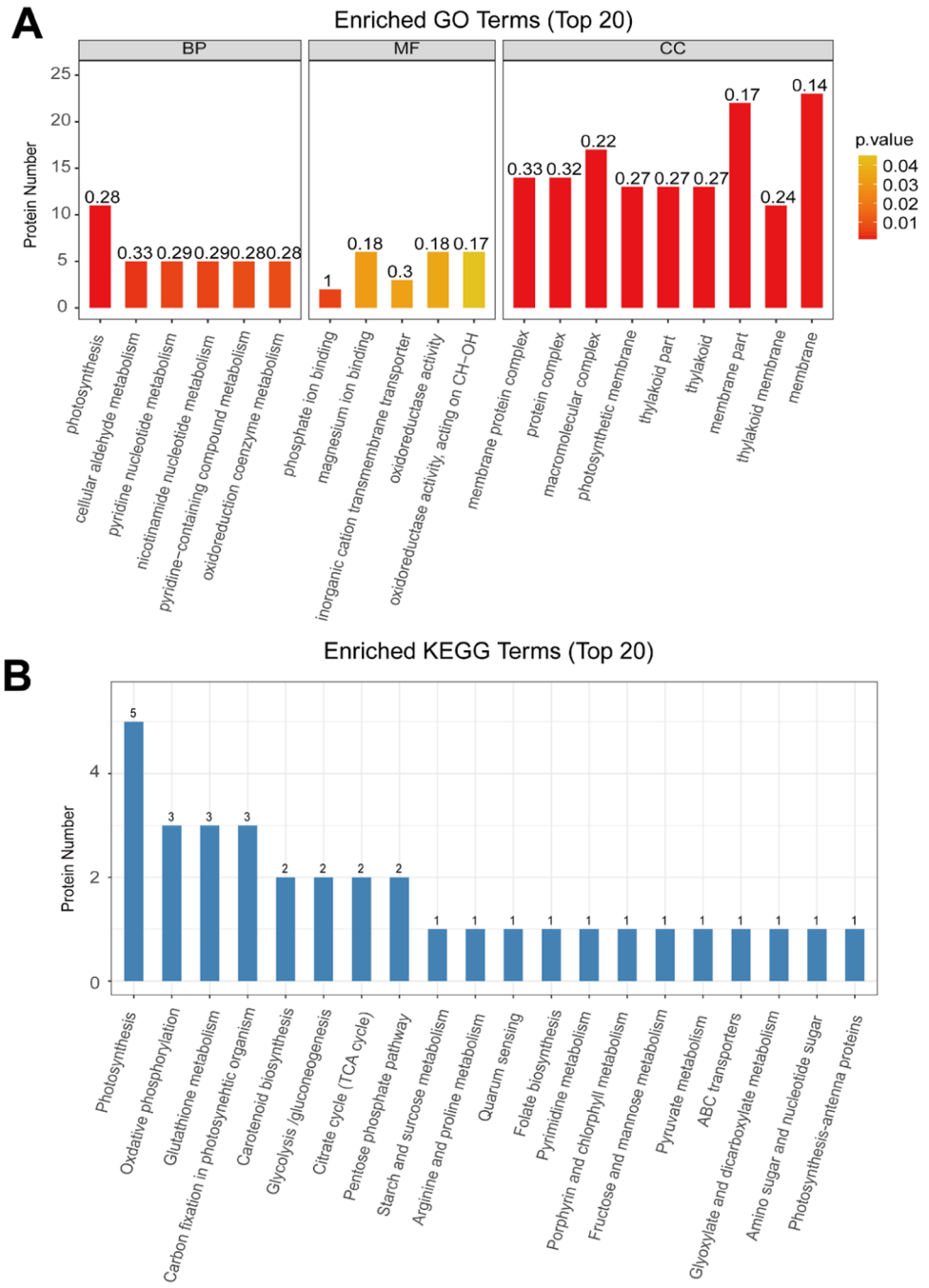


**Figure 5.** GO and KEGG analysis on differently abundant acetylated proteins (DAAPs) based on one-way ANOVA from different dehydration treatments. (A) GO analysis and (B) KEGG analysis.

levels of some DAAPs related to ATP synthase involved in the photosynthetic light reaction were upregulated, such as ATPB, ATP synthase A, and ATP synthase gamma, due to dehydration treatments. Interestingly, LysAc levels of many DAAPs related to the Calvin cycle were downregulated such as RbcS3, FBP1, and G3PDH under dehydration treatments (Figure 8 and Table S3). Dehydration treatments also induced decreased LysAc levels of some DAAPs involved in the ROS scavenging system, such as SOD and GST. In addition, dehydration treatments induced the LysAc levels, gene expression levels, and enzymes involved in glycogen metabolic pathways, such as *GLGX* (Figures S9A,4B,C, and8).

## DISCUSSION

### Protein Acetylation Regulates Photosynthesis in *N. flagelliforme*

Chemical modifications of photosynthetic proteins, such as the acetylation of lysine residues, have been reported extensively in higher plants[28] and the cyanobacterium.[13] However, fewer studies were reported about their function and their roles in photosynthetic response to various abiotic stresses. Our results also showed significant enrichment of acetylproteins involved in photosynthesis in *N. flagelliforme* exposed to dehydration treatments (Figure 5A). Notably, a total of 33 acetylproteins were involved in the photosynthetic pathway, including photosynthetic light reaction (including ATPB) and Calvin


https://doi.org/10.1021/acs.jproteome.1c00823
J. Proteome Res. 2022, 21, 482−493

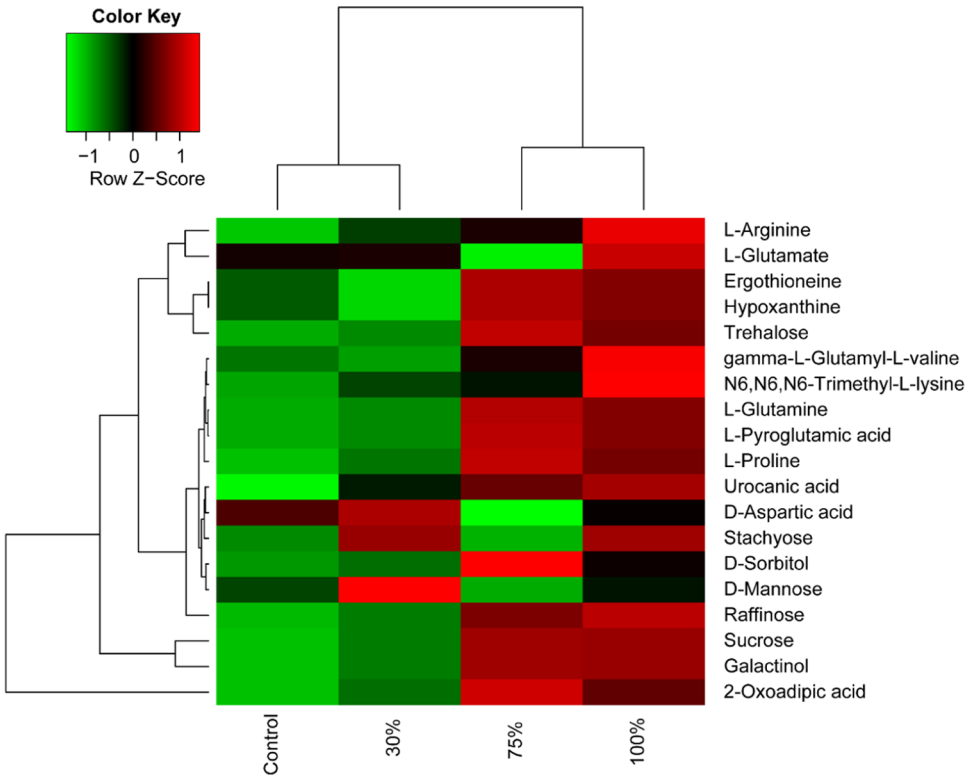


**Figure 6.** Metabolite contents related to amino acid and sucrose metabolism in *N. flagelliforme* exposed to different dehydration treatments.

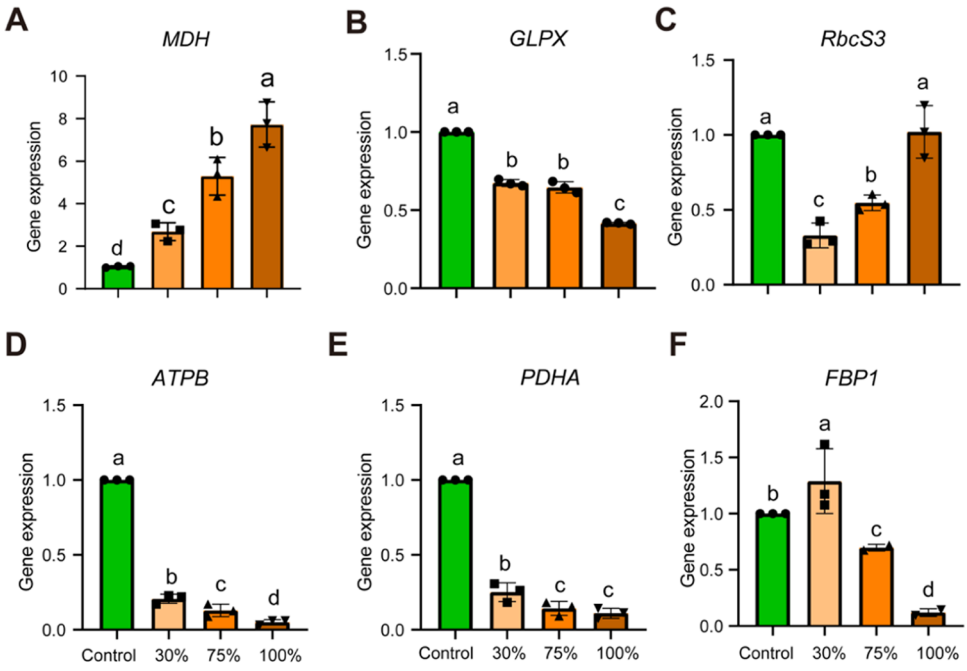


**Figure 7.** Relative expression levels of glutathione and photosynthetic metabolism in *N. flagelliforme* exposed to different dehydration treatments. (A−F) Malate dehydrogenase (MDH), fructose-bisphosphatase class II (GLPX), Rubisco small subunit 3 (RbcS3), ATP synthase subunit B (ATPB), pyruvate dehydrogenase (acetyl-transferring) E1 component subunit $\alpha$ (PDHA), and fructose-ibsphosphaease1 (FBP1). Different letters represent significant levels at $P < 0.05$ for the expression level of each gene among different dehydration treatments.

cycle (including Rubisco, Figure 8 and Table S2). Rubisco represents the most important light-regulated enzyme of carbon fixation, and its activity is documented to be negatively affected by LysAc levels.[16−18] There are many lysine residues of Rubisco that are responsible for catalyzed properties can be acetylated, such as Lys201, Lys252, and Lys334.[29] In this study, we reported 13 LysAc sites including Lys176 for RbcL (WP_100900845.1) that has not been reported previously.[16,18] This suggests that Rubisco acetylation could be very important for its function in the regulation of the photosynthetic process. This also supports the vital role of Lysine acetylome functions


https://doi.org/10.1021/acs.jproteome.1c00823
J. Proteome Res. 2022, 21, 482−493

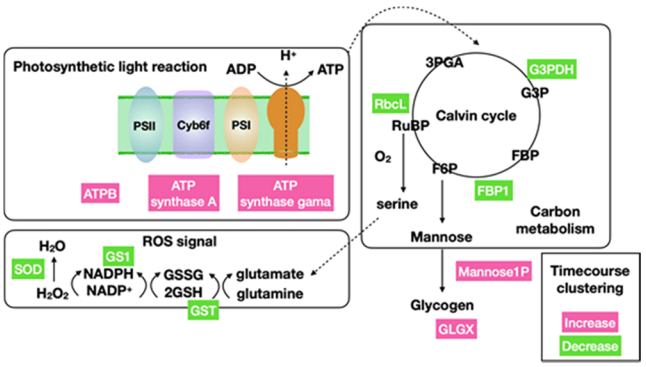


**Figure 8.** Proposed working model representing acetylation levels of proteins in *N. flagelliforme* exposed to different dehydration treatments. Pink and green boxes represent increased and decreased LysAc levels due to dehydration treatments, respectively. Some DAAPs related to the photosynthetic light reaction were upregulated, such as ATPB (WP_100899338.1), ATP synthase A (WP_100902985.1), and ATP synthase gamma (WP_100899334.1), due to dehydration treatments, whereas dehydration induced the inhibition of the Calvin cycle process, although ATP production is sufficient. Many DAAPs related to the Calvin cycle are downregulated as well such as RbcL (WP_100900845.1), FBP1 (WP_100899677.1), and G3PDH (WP_100900471.1). Dehydration treatment also causes the inhibition of the ROS scavenging system, such as decreased LysAc levels of SOD (WP_100897098.1), GS1 (WP_100900686.1), and GST (WP_100899636.1). In addition, the gene expression levels, enzymatic activities, and LysAc levels of glycogen metabolic pathways especially are enhanced under dehydration treatments.

of the cyanobacterium *Synechocystis* sp. PCC 6803 in photosynthesis regulation.[13]

Fructose-bisphosphate aldolase (EC 4.1.2.13, FBA) constitutes a pivotal enzyme for primary metabolism in plants and cyanobacterium species, playing very important roles in glycolysis metabolism in the cytoplasm, and in the Calvin cycle occurring in plastids.[30−32] In plants, FBA generally exists in two isoforms, a cytoplasmic form together with a chloroplastic form.[33−35] During the Calvin cycle, chloroplastic FBA catalyzes the targeted metabolites for starch production, while the FBA is expressed in cytosol functions in the sucrose biosynthesis and gluconeogenesis process.[30,36] Our study identified six FBA (WP_100901523.1) LysAc sites (Lys 257, Lys 26, Lys 244, Lys 132, Lys 214, and Lys 320) with different LysAc sites (Table S2), revealing that LysAc regulates the glycolytic signaling pathway in the cytoplasm as observed in higher plants.[37]

## Acetylated Proteins Involved in Glucose Metabolism

Except for the Calvin cycle, in line with previous knowledge on LysAc, various metabolic enzymes involved in multiple metabolic processes can also be acetylated, including the enzymes related to glycolysis/gluconeogenesis and the TCA cycle (Figure 5B and Table S2). A total of six acetylproteins involved in the TCA cycle were acetylated. In particular, the mitochondrial PDC, which connects glycolysis to the Krebs cycle and plays key roles in glucose homeostasis, consists of PDHA (WP_100898852.1), dihydrolipoamide dehydrogenase (WP_100899221), and dihydrolipoyl transacetylase (WP_100900857.1, Table S2). We identified four LysAc sites in PDHA, with decreased LysAc levels in response to dehydration stress of *N. flagelliforme* (Table S3). This is very likely due to the inhibitory effects of LysAc on PDHA as a subunit of PDH, consequently leading to negative regulation of PDC, as reported in mammal cells.[38] It also found similar results that increasing PDHA LysAc slightly decreased its enzyme activity in flooded *K. candel* leaves.[11] Interestingly, we found that expression levels of the *PDHA* gene were declined dramatically under both 30% and 75% dehydrated treatments (Figure 7E). Meanwhile, both the levels of LysAc of PDHC1 remain unchanged for these two treatments compared to control, suggesting that acetylation might have different effects on the activity of glycolysis enzymes.

## Protein Acetylation Regulation of the ROS Antioxidant System in the Dehydration Response

It is well reported that most of the abiotic stress events such as dehydration stress induced the production of oxidative stress through reactive oxygen species (ROS), consisting of superoxide free radical ($^{\bullet}O_2^-$), singlet oxygen ($^1O_2$), hydrogen peroxide ($H_2O_2$), and hydroxyl radical ($OH^{\bullet}$).[39] Acetylation of mitochondrial enzymes in the TCA cycle is an inhibitory indicator, which reflects that redox relevant metabolism can be inhibited by high acetylation levels among these central metabolic enzymes.[40] We observed that oxidoreductase processes were significantly enriched in the DAAPs (Figure 5A), and three proteins related to ROS scavenging systems, including SOD, GST, and GS1, were slightly or dramatically decreased together with their gene expression levels (Table S3 and Figure S9F−H), suggesting that ROS seems to have two-side effects under abiotic stress conditions that rely on their overall cellular amount.[39] Proline is among the compatible compounds and its level is a biomarker of different stressful conditions. The levels of proline facilitate the plants to promote stress tolerance capacities and enhance their antioxidant activity to detoxify the deleterious elements for the cell.[41] We observed increased proline content together with increased arginine produced from glutamate metabolism together with its following dehydration treatments in *N. flagelliforme* (Figure 6 and Table S4), supporting that ROS and the glutamate metabolic pathway represent a common physiological response in higher plants and the cyanobacterium exposed to various abiotic stresses.[42]

## Motif Analysis of LysAc Sites in *N. flagelliforme*

To map the specific amino acids surrounding the acetylated lysine (LysAc), we investigated the frequency of different amino acids around the acetylated lysine from −6(log 2) to +6(log 2). Among them, 11 conserved sequence motifs of the LysAc sites with a motif score >10 in *N. flagelliforme* were confidently identified (Figure 2B). As shown in Figure S3B, arginine (R) was highly enriched in the +1(log 2) position in *N. flagelliforme*, which was similar to *Synechocystis* sp. PCC 6803 site-specific LysAc motif. However, we also observed quite a different situation in *N. flagelliforme* LysAc compared with *Synechocystis* sp. PCC 6803 in another study.[13] We observed that leucine (L) was most commonly found at the +1(log 2) and +2(log 2) positions, whereas glutamate (E) appears more frequently at the −1(log 2) position. The differences in the LysAc motif in these organisms implicate the existence of different acyltransferases or deacylases in prokaryotes. In *E. coli*, glycine at the −1(log 2) position, alanine at the +1(log 2) position, and glutamic acid at the +5(log 2) position were overrepresented,[43] suggesting that acetylation of this protein might be important for its function.


https://doi.org/10.1021/acs.jproteome.1c00823
J. Proteome Res. 2022, 21, 482−493

## CONCLUSIONS

In this study, a dehydration treatment was applied in *N. flagelliforme*; as a result, we observed that starch contents were significantly accumulated and identified 2474 acetylpeptides in the whole proteome of *N. flagelliforme*, which provides the first comprehensive acetylome analysis of this important dehydration-tolerant species. Based on the integrative analysis of acetylome and metabolism, we found that the pathways of carbon metabolism and the ROS scavenging system were identified in the lists of both DAAPs and DAMs. In addition, LysAc levels of the proteins related to the two pathways were dramatically altered due to dehydration treatments. We hence emphasized the important functional roles of protein acetylation in the adaptive response for *N. flagelliforme* to such extreme dehydration environments.

## ASSOCIATED CONTENT

### Supporting Information

The Supporting Information is available free of charge at https://pubs.acs.org/doi/10.1021/acs.jproteome.1c00823.

(Figure S1) Distribution of the ion score and deviation of acetylpeptides; (Figure S2) Abundance of acetylpeptides and relative molecular weight; (Figure S3) Length of acetylpeptides and the frequency of acetylated sites of peptides; (Figure S4) Identified acetylpeptides and proteins in *N. flagelliforme* subjected to dehydration treatments; (Figure S5) Differentially abundant metabolites in *N. flagelliforme* subjected to 30% dehydration treatments relative to control; (Figure S6) Differentially abundant metabolites in *N. flagelliforme* subjected to 75% dehydration treatments relative to control; (Figure S7) Differentially abundant metabolites in *N. flagelliforme* subjected to 100% dehydration treatments relative to control; (Figure S8) Time course clustering analysis on acetylproteins in *N. flagelliforme* subjected to different dehydration treatments from 0 (control) to 100%; (Figure S9) Relative expression levels of genes involved in glutathione metabolism; (Figure S10) Protein−protein interactive (PPI) network of DAAPs related to sucrose metabolism and carbon metabolism (PDF)

(Table S1) List of primers listed in this study; (Table S2) Aceylpeptides identified in this study across different dehydration treatments in *N. flagelliforme*; (Table S3) Key differentially abundant lys-acetylated proteins (DAAPs) that involved in glutathione and carbon fixation metabolism; (Table S4) Differentially abundant metabolites in *N. flagelliforme* subjected to different dehydration treatments relative to control (XLSX)

(PDF)

(XLSX)

## AUTHOR INFORMATION


### Corresponding Author

**Wenyu Liang** − *School of Life Sciences, Ningxia University, Yinchuan 750021, P. R. China; Key Laboratory of Ministry of Education for Conservation and Utilization of Special Biological Resources in the Western China, Ningxia University, Yinchuan 750021, P. R. China*; Phone: +86-0951-2062810; Email: liang_wy@nxu.edu.cn; Fax: +86-0951-2062810

### Authors

**Lingxia Wang** − *School of Life Sciences, Ningxia University, Yinchuan 750021, P. R. China; Key Laboratory of Ministry of Education for Conservation and Utilization of Special Biological Resources in the Western China, Ningxia University, Yinchuan 750021, P. R. China*; orcid.org/0000-0002-1890-5460

**Xiaoxu Li** − *School of Life Sciences, Ningxia University, Yinchuan 750021, P. R. China*

**Meng Wang** − *School of Life Sciences, Ningxia University, Yinchuan 750021, P. R. China*

**Xiaorong Ma** − *School of Life Sciences, Ningxia University, Yinchuan 750021, P. R. China*

**Fan Song** − *School of Life Sciences, Ningxia University, Yinchuan 750021, P. R. China*

**Jinhong Hu** − *School of Life Sciences, Ningxia University, Yinchuan 750021, P. R. China*

**Wangli Liang** − *School of Life Sciences, Ningxia University, Yinchuan 750021, P. R. China*

Complete contact information is available at: https://pubs.acs.org/10.1021/acs.jproteome.1c00823


### Author Contributions

[§]L.W. and X.L. contributed equally to this work.

### Author Contributions

All data is available in the manuscript or the supplementary materials.

### Author Contributions

Conceptualization: W.L. and X.L.; methodology: M.W., X.M., F.S., J.H., and W.L.; investigation: M.W., X.M., F.S., J.H., and W.L.; writing: L.W. and W.L.; funding acquisition: L.W.; resources: L.W.; and Supervision: L.W. and W.L.

### Notes

The authors declare no competing financial interest.

## ACKNOWLEDGMENTS

This work was supported by the National Natural Science Grant of China (Award Nos. 31660114 and 31960060) and the Fourth Batch of Ningxia Youth Talents Supporting Program (Award No. NXTJ2019006). The authors would like to show great appreciation to Dr. Yaozong Wu (Sanshu Biotech. Co., LTD) for his contributions to the technical and experimental assistances in this study. They also thank Zhongkang Omics Biotech Company for its linguistic assistance during the preparation of this manuscript.

## REFERENCES

(1) Shen, Y.; Wei, W.; Zhou, D.-X. Histone Acetylation Enzymes Coordinate Metabolism and Gene Expression. *Trends Plant Sci.* **2015**, *20*, 614−621.

(2) Luo, M.; Cheng, K.; Xu, Y.; Yang, S.; Wu, K. Plant Responses to Abiotic Stress Regulated by Histone Deacetylases. *Front. Plant Sci.* **2017**, *8*, No. 2147.

(3) Filippakopoulos, P.; Knapp, S. Targeting Bromodomains: Epigenetic Readers of Lysine Acetylation. *Nat. Rev. Drug Discov.* **2014**, *13*, 337−356.

(4) Gil, J.; Ramírez-Torres, A.; Encarnación-Guevara, S. Lysine Acetylation and Cancer: A Proteomics Perspective. *J. Proteomics* **2017**, *150*, 297−309.

(5) Yang, X. J.; Seto, E. Lysine Acetylation: Codified Crosstalk with Other Posttranslational Modifications. *Mol. Cell* **2008**, *31*, 449−461.

(6) Allfrey, V. G.; Faulkner, R.; Mirsky, A. E. Acetylation and Methylation of Histones and Their Possible Role in the Regulation of RNA Synthesis. *Proc. Natl. Acad. Sci. U.S.A.* **1964**, *51*, 786−794.
(7) Norris, K. L.; Lee, J.-Y.; Yao, T.-P. Acetylation Goes Global: The Emergence of Acetylation Biology. *Sci. Signal.* **2009**, *2*, No. pe76.
(8) Guan, K.-L.; Xiong, Y. Regulation of Intermediary Metabolism by Protein Acetylation. *Trends Biochem. Sci.* **2011**, *36*, 108−116.
(9) Chen, Z.; Zhang, G.; Yang, M.; Li, T.; Ge, F.; Zhao, J. Lysine Acetylome Analysis Reveals Photosystem II Manganese-Stabilizing Protein Acetylation Is Involved in Negative Regulation of Oxygen Evolution in Model Cyanobacterium Synechococcus Sp. PCC 7002. *Mol. Cell. Proteomics* **2017**, *16*, 1297−1311.
(10) Altman-Price, N.; Mevarech, M. Genetic Evidence for the Importance of Protein Acetylation and Protein Deacetylation in the Halophilic Archaeon Haloferax Volcanii. *J. Bacteriol.* **2009**, *191*, 1610−1617.
(11) Pan, D.; Wang, L.; Chen, S.; Lv, X.; Lu, S.; Cheng, C.-L.; Tan, F.; Chen, W. Protein Acetylation as a Mechanism for *Kandelia Candel*'s Adaption to Daily Flooding. *Tree Physiol.* **2018**, *38*, 895−910.
(12) Nallamilli, B. R. R.; Edelmann, M. J.; Zhong, X.; Tan, F.; Mujahid, H.; Zhang, J.; Nanduri, B.; Peng, Z. Global Analysis of Lysine Acetylation Suggests the Involvement of Protein Acetylation in Diverse Biological Processes in Rice (*Oryza Sativa*). *PLoS One* **2014**, *9*, No. e89283.
(13) Mo, R.; Yang, M.; Chen, Z.; Cheng, Z.; Yi, X.; Li, C.; He, C.; Xiong, Q.; Chen, H.; Wang, Q.; Ge, F. Acetylome Analysis Reveals the Involvement of Lysine Acetylation in Photosynthesis and Carbon Metabolism in the Model Cyanobacterium *Synechocystis* Sp. PCC 6803. *J. Proteome Res.* **2015**, *14*, 1275−1286.
(14) Wang, Q.; Zhang, Y.; Yang, C.; Xiong, H.; Lin, Y.; Yao, J.; Li, H.; Xie, L.; Zhao, W.; Yao, Y.; Ning, Z.-B.; Zeng, R.; Xiong, Y.; Guan, K.-L.; Zhao, S.; Zhao, G.-P. Acetylation of Metabolic Enzymes Coordinates Carbon Source Utilization and Metabolic Flux. *Science* **2010**, *327*, 1004−1007.
(15) Choudhary, C.; Kumar, C.; Gnad, F.; Nielsen, M. L.; Rehman, M.; Walther, T. C.; Olsen, J. V.; Mann, M. Lysine Acetylation Targets Protein Complexes and Co-Regulates Major Cellular Functions. *Science* **2009**, *325*, 834−840.
(16) Finkemeier, I.; Laxa, M.; Miguet, L.; Howden, A. J. M.; Sweetlove, L. J. Proteins of Diverse Function and Subcellular Location Are Lysine Acetylated in Arabidopsis. *Plant Physiol.* **2011**, *155*, 1779−1790.
(17) Wu, X.; Oh, M.-H.; Schwarz, E. M.; Larue, C. T.; Sivaguru, M.; Imai, B. S.; Yau, P. M.; Ort, D. R.; Huber, S. C. Lysine Acetylation Is a Widespread Protein Modification for Diverse Proteins in *Arabidopsis*. *Plant Physiol.* **2011**, *155*, 1769−1778.
(18) Gao, X.; Hong, H.; Li, W. C.; Yang, L.; Huang, J.; Xiao, Y. L.; Chen, X. Y.; Chen, G. Y. Downregulation of Rubisco Activity by Non-Enzymatic Acetylation of RbcL. *Mol. Plant* **2016**, *9*, 1018−1027.
(19) Wang, L.; Lei, X.; Yang, J.; Wang, S.; Liu, Y.; Liang, W. Comparative Transcriptome Analysis Reveals That Photosynthesis Contributes to Drought Tolerance of *Nostoc Flagelliforme* (Nostocales, Cyanobacteria). *Phycologia* **2018**, *57*, 113−120.
(20) Liang, W.; Zhou, Y.; Wang, L.; You, X.; Zhang, Y.; Cheng, C.-L.; Chen, W. Ultrastructural, Physiological and Proteomic Analysis of *Nostoc Flagelliforme* in Response to Dehydration and Rehydration. *J. Proteomics* **2012**, *75*, 5604−5627.
(21) Wang, B.; Yang, L.; Zhang, Y.; Chen, S.; Gao, X.; Wan, C. Investigation of the Dynamical Expression of *Nostoc Flagelliforme* Proteome in Response to Rehydration. *J. Proteomics* **2019**, *192*, 160−168.
(22) Li, X.; Wang, L.; Wang, M.; Zhang, Z.; Ma, C.; Ma, X.; Na, X.; Liang, W. Global Analysis of Protein Succinylation Modification of *Nostoc Flagelliforme* in Response to Dehydration. *J. Proteomics* **2021**, *237*, No. 104149.
(23) Yin, H.; Xie, M.; Zhang, L.; Huang, J.; Xu, Z.; Li, H.; Jiang, R.; Wang, R.; Zeng, X. Identification of Sewage Markers to Indicate Sources of Contamination: Low Cost Options for Misconnected Non-Stormwater Source Tracking in Stormwater Systems. *Sci. Total Environ.* **2019**, *648*, 125−134.
(24) Bradford, M. M. A Rapid and Sensitive Method for the Quantitation of Microgram Quantities of Protein Utilizing the Principle of Protein-Dye Binding. *Anal. Biochem.* **1976**, *72*, 248−254.
(25) Götz, S.; García-Gómez, J. M.; Terol, J.; Williams, T. D.; Nagaraj, S. H.; Nueda, M. J.; Robles, M.; Talón, M.; Dopazo, J.; Conesa, A. High-Throughput Functional Annotation and Data Mining with the Blast2GO Suite. *Nucleic Acids Res.* **2008**, *36*, 3420−3435.
(26) Perez-Riverol, Y.; Csordas, A.; Bai, J.; Bernal-Llinares, M.; Hewapathirana, S.; Kundu, D. J.; Inuganti, A.; Griss, J.; Mayer, G.; Eisenacher, M.; Pérez, E.; Uszkoreit, J.; Pfeuffer, J.; Sachsenberg, T.; Yılmaz, Ş.; Tiwary, S.; Cox, J.; Audain, E.; Walzer, M.; Jarnuczak, A. F.; Ternent, T.; Brazma, A.; Vizcaíno, J. A. The PRIDE Database and Related Tools and Resources in 2019: Improving Support for Quantification Data. *Nucleic Acids Res.* **2019**, *47*, D442−D450.
(27) Livak, K. J.; Schmittgen, T. D. Analysis of Relative Gene Expression Data Using Real-Time Quantitative PCR and the $2^{-\Delta\Delta CT}$Method. *Methods* **2001**, *25*, 402−408.
(28) Koskela, M. M.; Brünje, A.; Ivanauskaite, A.; Grabsztunowicz, M.; Lassowskat, I.; Neumann, U.; Dinh, T. V.; Sindlinger, J.; Schwarzer, D.; Wirtz, M.; Tyystjärvi, E.; Finkemeier, I.; Mulo, P. Chloroplast Acetyltransferase NSI Is Required for State Transitions in *Arabidopsis Thaliana*. *Plant Cell* **2018**, *30*, 1695−1709.
(29) Gao, X.; Hong, H.; Li, W.-C.; Yang, L.; Huang, J.; Xiao, Y.-L.; Chen, X.-Y.; Chen, G.-Y. Downregulation of Rubisco Activity by Non-Enzymatic Acetylation of RbcL. *Mol. Plant* **2016**, *9*, 1018−1027.
(30) Li, D.; Han, X.; Tu, Q.; Feng, L.; Wu, D.; Sun, Y.; Chen, H.; Li, Y.; Ren, Y.; Wan, J. Structure-Based Design and Synthesis of Novel Dual-Target Inhibitors against Cyanobacterial Fructose-1,6-Bisphosphate Aldolase and Fructose-1,6-Bisphosphatase. *J. Agric. Food Chem.* **2013**, *61*, 7453−7461.
(31) Mininno, M.; Brugière, S.; Pautre, V.; Gilgen, A.; Ma, S.; Ferro, M.; Tardif, M.; Alban, C.; Ravanel, S. Characterization of Chloroplastic Fructose 1,6-Bisphosphate Aldolases as Lysine-Methylated Proteins in Plants. *J. Biol. Chem.* **2012**, *287*, 21034−21044.
(32) Nakahara, K.; Yamamoto, H.; Miyake, C.; Yokota, A. Purification and Characterization of Class-I and Class-II Fructose-1, 6- Bisphosphate Aldolases from the Cyanobacterium *Synechocystis* Sp. PCC 6803. *Plant and Cell Physiol.* **2003**, *44*, 326−333.
(33) Ma, S.; Martin-Laffon, J.; Mininno, M.; Gigarel, O.; Brugière, S.; Bastien, O.; Tardif, M.; Ravanel, S.; Alban, C. Molecular Evolution of the Substrate Specificity of Chloroplastic Aldolases/Rubisco Lysine Methyltransferases in Plants. *Mol. Plant* **2016**, *9*, 569−581.
(34) Bond, J. S.; Barrett, A. J. Degradation of Fructose-1, 6-Bisphosphate Aldolase by Cathepsin B. *Biochem. J.* **1980**, *189*, 17−25.
(35) Imanaka, H.; Fukui, T.; Atomi, H.; Imanaka, T. Gene Cloning and Characterization of Fructose-1,6-Bisphosphate Aldolase from the Hyperthermophilic Archaeon *Thermococcus Kodakaraensis* KOD1. *J. Biosci. Bioeng.* **2002**, *94*, 237−243.
(36) Simkin, A. J.; McAusland, L.; Headland, L. R.; Lawson, T.; Raines, C. A. Multigene Manipulation of Photosynthetic Carbon Assimilation Increases $CO_2$ Fixation and Biomass Yield in Tobacco. *J. Exp. Bot.* **2015**, *66*, 4075−4090.
(37) Xiong, Y.; Peng, X.; Cheng, Z.; Liu, W.; Wang, G.-L. A Comprehensive Catalog of the Lysine-Acetylation Targets in Rice (*Oryza Sativa*) Based on Proteomic Analyses. *J. Proteomics* **2016**, *138*, 20−29.
(38) Fan, J.; Shan, C.; Kang, H.-B.; Elf, S.; Xie, J.; Tucker, M.; Gu, T.-L.; Aguiar, M.; Lonning, S.; Chen, H.; Mohammadi, M.; Britton, L.-M. P.; Garcia, B. A.; Alečković, M.; Kang, Y.; Kaluz, S.; Devi, N.; Van Meir, E. G.; Hitosugi, T.; Seo, J. H.; Lonial, S.; Gaddh, M.; Arellano, M.; Khoury, H. J.; Khuri, F. R.; Boggon, T. J.; Kang, S.; Chen, J. Tyr Phosphorylation of PDP1 Toggles Recruitment between ACAT1 and SIRT3 to Regulate the Pyruvate Dehydrogenase Complex. *Mol. Cell* **2014**, *53*, 534−548.


https://doi.org/10.1021/acs.jproteome.1c00823
*J. Proteome Res.* 2022, 21, 482−493

(39) Cruz de Carvalho, M. H. Drought Stress and Reactive Oxygen Species: Production, Scavenging and Signaling. *Plant Signal. Behav.* **2008**, *3*, 156−165.
(40) Baeza, J.; Smallegan, M. J.; Denu, J. M. Mechanisms and Dynamics of Protein Acetylation in Mitochondria. *Trends Biochem. Sci.* **2016**, *41*, 231−244.
(41) Li, J.; Jemaa, E.; Shang, C.; Zhang, H.; Zhu, X.; Yu, J.; Chen, G.; Qu, M.; Sun, D. Combined Proteomics and Metabolism Analysis Unravels Prominent Roles of Antioxidant System in the Prevention of Alfalfa (*Medicago Sativa* L.) against Salt Stress. *Int. J. Mol. Sci.* **2020**, *21*, No. 909.
(42) Kaur, G.; Asthir, B. Proline: A Key Player in Plant Abiotic Stress Tolerance. *Biol. Plant.* **2015**, *59*, 609−619.
(43) Schilling, B.; Basisty, N.; Christensen, D. G.; Sorensen, D.; Orr, J. S.; Wolfe, A. J.; Rao, C. V. Global Lysine Acetylation in *Escherichia Coli* Results from Growth Conditions That Favor Acetate Fermentation. *J. Bacteriol.* **2019**, *201*, No. e00768.


https://doi.org/10.1021/acs.jproteome.1c00823
*J. Proteome Res.* 2022, 21, 482−493